

**Quasi-two-dimensional excitons in (Zn,Cd)Se/ZnSe quantum wells:  
Reduced exciton-LO-phonon coupling due to confinement effects**

N. T. Pelekanos, J. Ding, M. Hagerott, and A. V. Nurmikko

*Division of Engineering and Department of Physics, Brown University, Providence, Rhode Island 02912*

H. Luo, N. Samarth, and J. K. Furdyna

*Department of Physics, University of Notre Dame, Notre Dame, Indiana 46556*

(Received 21 June 1991; revised manuscript received 21 October 1991)

Quasi-two-dimensional (2D) excitons in (Zn,Cd)Se/ZnSe quantum wells were investigated. We observed a confinement-induced enhancement of the exciton binding energy to a value greater than the longitudinal-optical (LO) -phonon energy. This unusual condition results in an effective reduction of the exciton-LO-phonon coupling. As a consequence, excitonic absorption features in this quantum-well system are well preserved to room temperature and beyond.

Very recently there have been major developments with wide-band-gap II-VI compound semiconductors toward the realization of semiconductor optoelectronic devices in the blue-green region of the optical spectrum, culminating in the demonstration of a diode laser.<sup>1</sup> Part of the success in allowing for this breakthrough is due to the identification of the (Zn,Cd)Se/ZnSe quantum well (QW) as a particularly useful heterostructure for electron-hole pair confinement.<sup>2</sup> A key observation leading to this identification was the observation of well-defined exciton absorption features at room temperature.<sup>2</sup> In the III-V compound semiconductors, the role of two-dimensional electron-hole confinement in enhancing the exciton binding energy and oscillator strength is now very well understood.<sup>3</sup> For example, well-defined exciton-related absorption features from GaAs/(Ga,Al)As multiple-quantum wells (MQW's) are preserved at room temperature, in spite of the relatively short exciton lifetime (< 1 psec) due to scattering events with longitudinal-optical (LO) phonons. The situation in the more polar II-VI compounds is considerably more challenging due to the much stronger coupling with the LO phonons. In Fig. 1 we give a simplified schematic illustration of the major processes that contribute to the phonon-induced lifetime of the lowest lying exciton near room temperature: by absorbing one LO phonon of energy  $\hbar\omega_{LO}$  via the Fröhlich interaction, a  $1S(\mathbf{q}\approx 0)$  exciton either dissociates into the free electron-hole continuum or scatters within the discrete exciton bands. (We consider the acoustic-phonon contribution separately below.) It is important to notice that the former process requires that the exciton binding energy is smaller than  $\hbar\omega_{LO}$ . The lifetime broadening [full width at half maximum (FWHM)] induced to the  $1S(0)$  state by one LO phonon scattering can be written within first-order perturbation theory as<sup>4</sup>

$$\Gamma(T) = \Gamma_{inh} + \Gamma_{LO} [\exp(\hbar\omega_{LO}/k_B T) - 1]^{-1}, \quad (1)$$

where  $\Gamma_{inh}$  is the linewidth of inhomogeneous origin, and  $\Gamma_{LO}$  represents the strength of the exciton-LO phonon coupling and can be expressed as

$$\Gamma_{LO} = 2\pi V \sum_{\lambda} \int d^3q (2\pi)^{-3} |V_{\lambda,1S}(\mathbf{q})|^2 \times \delta(E_{1S} - E_{\lambda}(\mathbf{q}) + \hbar\omega_{LO}(\mathbf{q})); \quad (2)$$

here  $\lambda$  runs over all final exciton states of energy  $E_{\lambda}(\mathbf{q})$  and wave vector  $\mathbf{q}$ , and  $V_{\lambda,1S}(\mathbf{q})$  is the matrix element of the Fröhlich Hamiltonian for the transition from  $E_{1S}$  to  $E_{\lambda}(\mathbf{q})$ . As is well known,  $\Gamma_{LO}$  increases with the polarity of the material. As an example of this hierarchy, the values for bulk GaAs, ZnTe, and ZnSe are 10, 30, and 60 meV, respectively. This accounts for the fact that the exciton absorption features for bulk ZnSe disappear at  $T \approx 200$  K in spite of the larger exciton binding energy and oscillator strength compared with GaAs. The key aspect of the problem at hand, however, is that the bulk exciton rydberg in ZnSe is approximately 17 meV whereas the LO-phonon energy  $\hbar\omega_{LO} \approx 31$  meV. Therefore in a properly designed quantum-well structure the possibility exists for the quasi-2D (where 2D denotes two

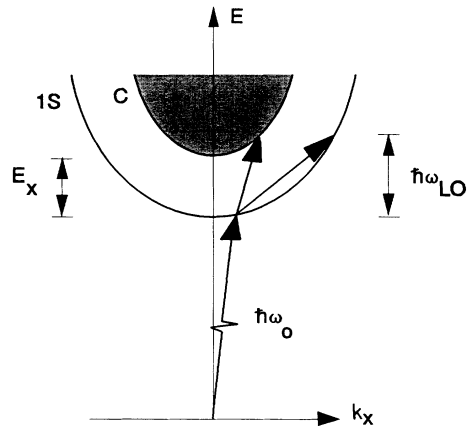


FIG. 1. Schematic illustration of the major processes (arrows) contributing to the phonon induced lifetime of the lowest-lying exciton. The shaded area represents continuum states.

dimensional) exciton rydberg to reach a value  $\mathcal{R}_y^* \geq \hbar\omega_{\text{LO}}$ . We would like to stress that this cannot occur in a GaAs-based system where the bulk exciton binding energy is approximately 5 meV and  $\hbar\omega_{\text{LO}}=36$  meV. In this circumstance that has not to our knowledge been encountered in earlier work with exciton absorption in semiconductor QW's, the exciton dissociation channel would be inhibited and a subsequent reduction of the exciton-LO-phonon coupling would occur; hence one may expect to observe room-temperature excitons in a ZnSe-based MQW system. Nonetheless, in earlier work, e.g., with ZnSe/(Zn,Mn)Se MQW's,<sup>5</sup> the exciton absorption features typically disappeared at about 200 K (as in the bulk), most likely due to the weak valence-band confinement which keeps the exciton closer to the three-dimensional than to the two-dimensional limit. This "asymmetry" in the electron-hole confinement has been a general problem with several wide-band-gap II-VI heterostructures.

In this paper, we report on the characterization of stable room-temperature quasi-2D excitons in (Zn,Cd)Se/ZnSe MQW's (following an initial report<sup>2</sup>) and present detailed experimental evidence that this is due to confinement effects. Our structures were grown by molecular-beam epitaxy (MBE) on [100]-oriented nearly lattice-matched GaAs substrates, following the deposition of a 2- $\mu\text{m}$  thick ZnSe buffer layer. A ZnSe cap layer of about 2000 Å was grown on top of the MQW segment. Details of the MBE growth are given elsewhere.<sup>6</sup> The MQW segment typically consisted of several QW's of  $\text{Zn}_{1-x}\text{Cd}_x\text{Se}$  with alloy concentration  $x=0.25-0.30$ , and of QW thickness ranging from 30 to 200 Å. The QW's are separated by 500 Å of ZnSe barrier layer. The total thickness of the QW section was kept small (a few hundred Å) to reduce the probability for the formation of misfit dislocations originating from the (Zn,Cd)Se/ZnSe lattice mismatch ( $\approx 1.6\%$ ). Thus, we attempted to secure that the structures remained in the pseudomorphic regime, with all the strain accommodated in the QW layers. Experimental indication that the structures were indeed pseudomorphic came from resonant Raman spectroscopy. By this technique, we measured the value of  $\hbar\omega_{\text{LO}}$  in the alloy QW material to be 31.8 meV at  $T=10$  K for a sample with 6 QW's of 30 Å width ( $6 \times 30$  Å) and Cd concentration  $x=0.25$ , by tuning the photon energy of excitation into resonance with the  $n=1$  exciton level of the QW. This value deviates significantly from the LO-phonon energy of  $\text{Zn}_{0.75}\text{Cd}_{0.25}\text{Se}$  which at low temperatures is approximately 30.8 meV (Ref. 7), (note that the  $\text{Zn}_{1-x}\text{Cd}_x\text{Se}$  system exhibits one mode behavior). The deviation is explained by noting that the expected in-plane strain between ZnSe and  $\text{Zn}_{1-x}\text{Cd}_x\text{Se}$  of  $x=0.25$  is  $\epsilon \approx -1.6\%$ . If we assume that all the strain in the samples is accommodated in the QW layers and apply the standard approach<sup>8</sup> for strain-induced Raman shifts with material constants of ZnSe [as constants for (Zn,Cd)Se are not available], we obtain

$$\omega_{\text{LO}}(\epsilon) = \omega_{\text{LO}}(0) + 2\Delta\Omega_H - \frac{2}{3}\Delta\Omega, \quad (3)$$

where

$$\Delta\Omega_H = \frac{p+2q}{6\omega_{\text{LO}}^2(0)} \frac{S_{11}+2S_{12}}{S_{11}+S_{12}} \epsilon\omega_{\text{LO}}(0),$$

$$\Delta\Omega = \frac{p-q}{2\omega_{\text{LO}}^2(0)} \frac{S_{11}-S_{12}}{S_{11}+S_{12}} \epsilon\omega_{\text{LO}}(0), \quad (4)$$

where the  $S_{ij}$  are the compliance constants ( $S_{11}+2S_{12}=0.57, S_{11}-S_{12}=3.11$ ), and  $(p+2q)/6\omega_{\text{LO}}^2(0)$  and  $(p-q)/2\omega_{\text{LO}}^2(0)$  represent the deformation constants ( $-1.8 \pm 0.4$  and  $0.62 \pm 0.2$ , respectively). This yields  $\omega_{\text{LO}}(\epsilon) = \omega_{\text{LO}}(0)[1 - (2.35 \pm 0.4)\epsilon]$  so that from the experimentally measured  $\omega_{\text{LO}}(\epsilon) = 31.8$  meV we obtain the strain in the quantum well to be  $\epsilon \approx -(1.4 \pm 0.2)\%$ , very near the expected pseudomorphic limit. Recent work with a nearly lattice-matched (Zn,Cd)Se/(Zn,Mn)Se QW system by magneto-optical spectroscopy<sup>9</sup> indicated the presence of relatively small though potentially useful valence-band offsets, approximately 30 meV. This result would likely be approximately valid for the (Zn,Cd)Se/ZnSe system as well, in the absence of strain. However, we emphasize that the presence of the biaxial compressive strain in the (Zn,Cd)Se QW material has the type-I enhancing effect of further confining the heavy hole (HH), by increasing the HH valence-band potential barrier. A simple estimate is obtained by calculating the effect of the biaxial strain  $\epsilon$  in splitting the HH-LH degeneracy, as follows:<sup>10</sup>

$$\delta E_{\text{HH}} = a_v \frac{\delta V}{V} - \frac{1}{2} \delta E_{001}$$

$$\delta E_{\text{LH}} = a_v \frac{\delta V}{V} - \frac{\Delta_0}{2} + \frac{1}{4} \delta E_{001}$$

$$+ \frac{1}{2} [\Delta_0^2 + \Delta_0 \delta E_{001} + \frac{9}{4} (\delta E_{001})^2]^{1/2}, \quad (5)$$

where  $a_v$  is the valence-band hydrostatic deformation potential,  $\Delta_0$  ( $\approx 0.43$  eV) the spin-orbit splitting,  $\delta V/V = 2\epsilon(1 - C_{12}/C_{11})$  is the change in unit-cell volume, and  $\delta E_{001} = -2b\epsilon[(2C_{12} + C_{11})/C_{11}]$  is the uniaxial energy correction. The  $C_{ij}$  are the elastic constants and  $b$  the shear deformation potential. In these estimates we used  $a_v = 1.54$  eV,  $b = -1.17$  eV,  $C_{11} = 0.789$ , and  $C_{12} = 0.498$  as extrapolated from ZnSe values for a Cd concentration  $x=0.25$ . For  $\epsilon = -1.6 \times 10^{-2}$  we obtain  $\delta E_{\text{HH}} = +25$  meV whereas  $\delta E_{\text{LH}} = -52$  meV. These values, under the assumption that the unstrained valence-band offsets are approximately 30 meV, imply that the confining potential barrier for HH's under the effect of strain increases at least to 55 meV whereas the LH band alignment forms a weakly type-II superlattice. These considerations are important in understanding how this heterostructure can provide such robust quasi-2D HH excitons of  $\mathcal{R}_y^* \approx 40$  meV, as will be shown next.

In Fig. 2 the temperature-dependent absorption spectra for two MQW samples of different QW layer thickness is shown. The samples consist of several periods of  $\text{Zn}_{0.75}\text{Cd}_{0.25}\text{Se}$  QW's embedded in ZnSe barrier material, with QW width of 200 Å (left-hand panel) and 30 Å (right-hand panel). Strong  $n=1$  HH exciton features dominate the low-temperature spectra of both samples (absorption coefficients of the order of  $10^5 \text{ cm}^{-1}$  were

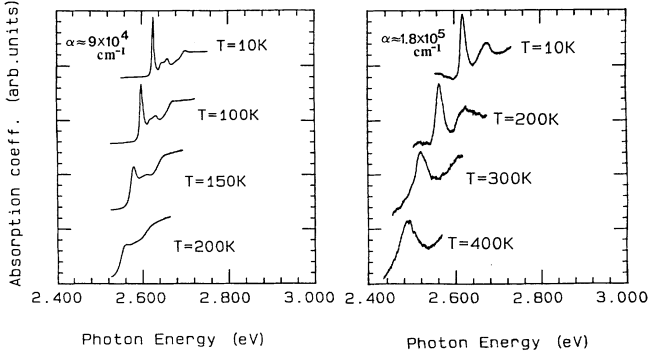


FIG. 2. Absorption coefficient of (Zn,Cd)Se/ZnSe MQW samples with well thickness  $L_w=200$  Å (left-hand panel) and  $L_w=30$  Å (right-hand panel), as a function of temperature. The peak values of the absorption coefficient are also indicated.

measured). Note, however, that the low-temperature value of the exciton linewidth  $\Gamma_{inh}$ , of inhomogeneous origin, is distinctly different for the two samples:  $\Gamma_{inh}=5$  and 13 meV for 200 Å and 30 Å QW widths, respectively. Two predominant mechanisms of inhomogeneous broadening are of relevance here: alloy concentration fluctuations and monolayer-type interface roughness. The latter mechanism affects mainly the narrower QW sample.<sup>11</sup> For example, we calculated this effect on the  $n=1$  confined electron-energy level,  $\Delta E_{1ML}$ , when the QW layer thickness is varied by 1 monolayer. For the sample with  $L_w=30$  Å,  $\Delta E_{1ML} \approx 10$  meV whereas for the sample with  $L_w=200$  Å,  $\Delta E_{1ML} \approx 0.5$  meV. Thus to explain the linewidth of the wider well 3D-like sample we must also consider the effect of the alloy fluctuations. To obtain a rough estimate of this effect we employ a model of a 3D Wannier exciton in a completely random mixed crystal<sup>12</sup> which yields

$$\Gamma_{inh} = \left[ 8 \ln 2 \left( \frac{dE}{dx} \right)^2 x(1-x)(V_0/V_1) \right]^{1/2}, \quad (6)$$

where  $x$  is the average alloy concentration ( $x=0.25$ ) and  $(dE/dx)$  is the derivative of the exciton energy as a function of concentration  $x$  [ $(dE/dx) \approx 900$  meV].  $V_0/V_1$  is the ratio of the unit cell and the exciton volumes. For an exciton radius of 40 Å, the alloy fluctuation contribution to the exciton linewidth is estimated to be approximately 7 meV which explains the observed broad QW linewidth, within the accuracy of the input parameters at least semi-quantitatively.

The most important observation that can be made from Fig. 2 is the striking contrast of the temperature dependence of the absorption spectra for the two samples. Given that the exciton Bohr diameter in bulk ZnSe is approximately 80 Å, the excitonic absorption peak of the sample with  $L_w=200$  Å corresponds to a quasi-3D exciton. The dominant  $n=1$  HH transition does indeed disappear at about 200 K, in a manner similar to bulk ZnSe samples. However, for the sample with  $L_w=30$  Å the situation is drastically altered. The quasi-2D exciton absorption peak remains distinct at temperatures well beyond room temperature ( $T > 400$  K). In Fig. 3 we plot

the exciton linewidth of this sample as a function of temperature. The solid line that passes through the data points is a fit with Eq. (1) with the further inclusion of acoustic-phonon scattering. This contribution has been considered by Lee, Koteles, and Vassell for GaAs/(Ga,Al)As QW's where it adds sizably to the exciton linewidth for temperatures approximately below  $T=150$  K.<sup>13</sup> By using the formulation of these authors, we find that the exciton-acoustic deformation-potential scattering and the piezoelectric scattering make a minor contribution to the linewidth in the (Zn,Cd)Se/ZnSe case, typically up to 2 meV. In adding the acoustic-phonon contribution to the fit in Fig. 3, we used the following parameters of ZnSe:  $m_e=0.16m_0$ ,  $m_{HH}=0.60m_0$ ,  $\epsilon=9.2$ ,  $\rho=5.264$  g/cm<sup>3</sup>,  $u=4.07 \times 10^5$  cm/sec,  $|h^{(e)}-h^{HH}|=0.049$  C/cm<sup>2</sup>, and  $|E_c-E_v|=5.82$  eV, where  $m_e(m_{HH})$  is the mass of the electron (heavy hole),  $\epsilon$  is the dielectric constant,  $\rho$  is the mass density,  $u$  is the acoustic velocity,  $h^{(e)}$  ( $h^{HH}$ ) is the piezoelectric constant for the electron (heavy hole), and  $E_c$  and  $E_v$  are the deformation potentials for the conduction and valence bands, respectively. The best fit is obtained for the parameter values  $\Gamma_{inh}=13$  meV and  $\Gamma_{LO}=25$  meV. As a comparison we also plot Eq. (1) for  $\Gamma_{inh}=13$  meV and  $\Gamma_{LO}=60$  meV, the latter being the low end for available values in bulk ZnSe, including our own measurements. We summarize the experimental values of  $\Gamma_{LO}$  for different QW widths in Table I. Notice that the  $\Gamma_{LO}$  for the 200 Å wide (Zn,Cd)Se QW's is larger than the bulk ZnSe value. This is somewhat puzzling but a similar effect was also observed in the (In,Ga)As-GaAs alloy containing QW system.<sup>14</sup> From Table I it is clear that with decreasing well thickness there is a drastic reduction (up to a factor of 3) in the exciton-phonon coupling, as expressed through  $\Gamma_{LO}$ . Similar studies in the GaAs-based systems have reported relatively small effects on the  $\Gamma_{LO}$  as one goes from the 3D to the 2D limit, for example, a linewidth change from 14 to 11 meV in Ref. 15. We interpret the strong reduction in the exciton-phonon coupling as being a manifestation of the fact that for the narrow QW's we have reached the condition  $\mathcal{R}_y^* \geq \hbar\omega_{LO}$ , so

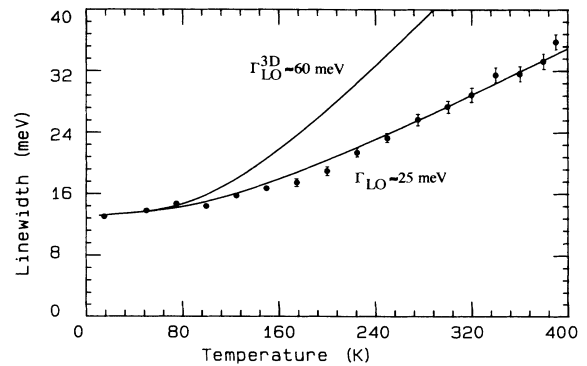


FIG. 3. Temperature dependence of the linewidth of the  $n=1$  HH exciton absorption peak of MQW sample with  $L_w=30$  Å. The solid lines are derived from Eq. (1) plus a contribution from acoustic-phonon scattering, for different values of the parameter  $\Gamma_{LO}$ .

TABLE I. List of experimental values of  $\Gamma_{LO}$  for different MQW samples with varying QW width.

QW width ( $\text{\AA}$ )	$\Gamma_{LO}$ (meV)
200	90
90	42
60	38
30	25
Bulk ZnSe	$\geq 60$

that according to the schematic of Fig. 1, the dissociation channel of excitons into the continuum states by 1-LO-phonon absorption is inhibited, resulting in an effective reduction of  $\Gamma_{LO}$ . The LO-phonon-mediated scattering to the 1S and excited states remain, however, but have substantially smaller cross sections.

Further supporting evidence that the exciton binding energy of our quasi-2D excitons exceeds  $\hbar\omega_{LO}$  was inferred from magnetoabsorption experiments in magnetic fields up to 24 T. The results that we will discuss here are all obtained from a  $6 \times 90 \text{\AA}$  sample. In the inset of Fig. 4 we plot the magnetoabsorption spectrum of this sample at 23.5 T. In addition to the main 1S  $n=1$  HH exciton peak, we identify the smaller absorption peak as due to the 2S  $n=1$  HH excited exciton state. This identification becomes more obvious when we plot the energy shift of the “2S” peak as a function of magnetic field in the figure. Although at low magnetic fields the shift is small and comparable to the 1S exciton diamagnetic shift, for  $B \geq 10$  T the shift becomes almost linear with the magnetic field. For  $B = 23.5$  T this blueshift is six times larger than the one for the 1S exciton. Such behavior rules out other possible assignments of the “2S” peak.

Specifically, the idea of a Landau level consisting of uncorrelated quasiparticles is eliminated from the low-field behavior. Also the possibility involving LH (light hole)  $n=1$  excitons is excluded by the consideration of the strain induced HH-LH splitting that was calculated above to be larger than 90 meV. On the other hand, we will now show that the 2S assignment is consistent with the calculations of Akimoto and Hasegawa<sup>16</sup> for two-dimensional excitons. First recall that the Bohr radius of the  $n$ th excited 3D exciton state is  $r_n = n^2 a_0$ , with  $n = 1, 2, \dots$ , where  $a_0 \simeq 40 \text{\AA}$  for ZnSe. Therefore for a QW of 90  $\text{\AA}$  well width, the 2S state is quasi two-dimensional. In the results of reference 16, two regimes are distinguished. For low fields, the energy position of the  $n$ th excited 2D magnetoexciton state is given by

$$E_n = -\frac{\mathcal{R}_y^0}{(n+1/2)^2} + \frac{5}{32}(n+\frac{1}{2})^4 \frac{(\hbar\omega_c)^2}{\mathcal{R}_y^0}, \quad (7)$$

where the band-gap energy is taken as the zero-energy point, the index  $n=0, 1, 2, \dots$ ,  $\mathcal{R}_y^0$  is the 3D value of the exciton binding energy [ $\simeq 17$  meV (Ref. 17)] and  $\hbar\omega_c$  is the cyclotron frequency explicitly dependent on the two-dimensional in-plane exciton reduced mass, for a magnetic field along the  $z$  axis. For high fields the magnetic-field dependence becomes sublinear

$$E_n = (n+1/2)\hbar\omega_c - \frac{3}{2} \left[ \frac{\mathcal{R}_y^0 \hbar\omega_c}{n+\frac{1}{2}} \right]^{1/2} + \text{const.} \quad (8)$$

As the extrapolated marker for the high-field regime, we can use the cyclotron frequency for which the  $n$ th exciton level crosses the  $E=0$  line. This is a strong function of  $n$  and for 1S is  $24\mathcal{R}_y^0 \simeq 408$  meV whereas for 2S is only  $0.9\mathcal{R}_y^0 \simeq 15$  meV. By applying the band masses and Lut-

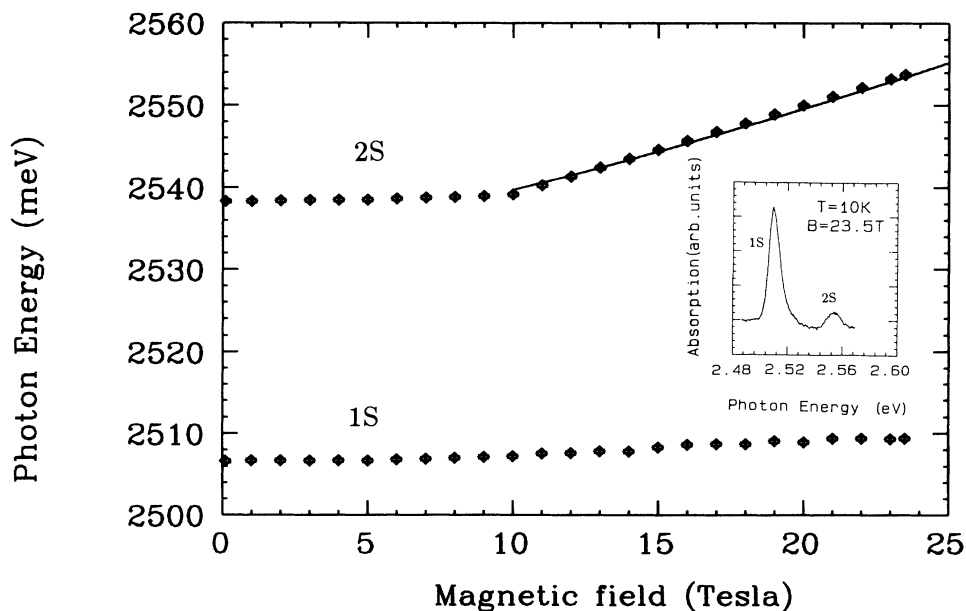


FIG. 4. Energy positions of the 1S and 2S  $n=1$  HH exciton states in a sample with well width 90  $\text{\AA}$ , as a function of magnetic field. The solid line is a theoretical fit. In the inset of magnetoabsorption spectrum of the same sample at 23.5 T is shown.

tiger parameters as determined in Ref. 17 for bulk ZnSe ( $m_e=0.147m_0, \gamma_1=2.45, \gamma_2=0.61, \gamma_3=1.11$ ) to the standard theory for nonparabolic in-plane bands in a QW,<sup>18</sup> we obtain for the 2D in-plane HH mass  $m_{\text{HH}}^\perp=0.34m_0$  and for the in-plane reduced exciton mass  $\mu^\perp \simeq 0.103m_0$  (the bulk value of  $\mu_0^\perp \simeq 0.135m_0$ ). Then the cyclotron frequency is  $\hbar\omega_c=1.125\text{meV/T}$  and it follows that the magnetic field beyond which the exciton level acquires a sublinear Landau-like magnetic-field dependence is for the 1S exciton, approximately 360 T, whereas for 2S exciton only 13.5 T, in very good agreement with our results (Fig. 4). To check the consistency of our interpretation further, we calculate the energy shift of the 2S exciton from 10 to 30 T using Eq. (8), with no other adjustable parameters except a constant term which is fixed so that the experimental value at 13 T is reproduced. The result of the calculation is plotted as a solid line in Fig. 4, and within experimental errors matches our data points very well.

The identification of the 2S-exciton state enables an accurate measurement of the quasi-2D exciton binding energy. Specifically, the difference between the zero-field 1S and 2S exciton energies is measured to be 31 meV. For 3D excitons  $|E_{1S}-E_{2S}|=0.75\mathcal{R}_y^0$  whereas for 2D excitons  $|E_{1S}-E_{2S}|=0.88\mathcal{R}_y^{2D}$ . We conclude that the binding energy of the quasi-2D exciton in the (Zn,Cd)Se/ZnSe QW sample with well thickness  $L_w=90\text{ \AA}$  is

$$35\text{ meV} \leq \mathcal{R}_y^* \leq 41\text{ meV} \quad (9)$$

a value which is larger than the  $\hbar\omega_{\text{LO}}=31.8\text{ meV}$ . For narrower QW's, the binding energy is expected to be further enhanced, validating our interpretation of the "quenched" temperature-dependent linewidth broadening. As a comparison we calculated the HH-exciton binding energy using a standard variational approach<sup>19</sup> for a QW width of 90 Å, confining barrier of 300 meV, valence-band-offset of 50 meV, and ZnSe material parameters<sup>17</sup> ( $\epsilon=9.2$ , and effective masses as given above). The outcome of this particular calculation gives for the HH-exciton binding energy an estimate of only about 30 meV. A possible account for the somewhat large discrepancy could be (apart from a poor variational approach) due to the finite effect on the exciton binding energy on the dielectric constant discontinuity in the heterostructure.<sup>20</sup> In light of this magneto-optical determination of the 1S-2S exciton energy difference and exciton binding energy in a sample with QW width of 90 Å, one gains better understanding of the results listed in Table I. As one goes from QW width  $L_w=200\text{ \AA}$  to  $L_w=90\text{ \AA}$  the exciton binding energy exceeds  $\hbar\omega_{\text{LO}}$  and the dissociation channel of 1S excitons into the continuum states is inhibited. Nonetheless, the transition from 1S to 2S excitons is still possible since the 1S-2S energy difference is less than  $\hbar\omega_{\text{LO}}$ . However, by decreasing the QW width further, the exciton binding energy is enhanced and the energy separation between 1S and 2S becomes gradually less accessible. We suggest that this explains the further reduction of  $\Gamma_{\text{LO}}$  as one goes from 90 to 60 Å and 30-Å QW widths.

Finally, we turn our attention to the effect of weak dis-

order on the radiative recombination of these quasi-2D excitons. In our system, the weak disorder originates from the alloy composition fluctuations and the interface roughness. Understanding the relaxation dynamics of excitons in the disorder-induced density-of-states tail would be very valuable in interpreting the recent observation of gain and laser action at these weakly localized exciton states from detailed optical pumping studies.<sup>21</sup> For our  $6 \times 90\text{-\AA}$  QW sample, at  $T \simeq 10\text{ K}$ , the photoluminescence (PL) peak resides on the low-energy tail of the inhomogeneously broadened exciton absorption peak ( $\Gamma_{\text{inh}} \simeq 9\text{ meV}$ ). The observed "Stokes shift" between absorptive and emissive resonance, a measure of the exciton localization energy, is about 6 meV, and is characteristic of weakly disordered systems. Similar shifts have been observed for all of our samples. To gain some insight into the length-scales of the exciton localization in our system, we studied the PL spectra in magnetic fields up to 12 T. In particular, we made use of the fact that the weak 1-LO phonon sideband of the exciton PL peak can be used as a probe of localized excitons in quantum-well systems.<sup>22,23</sup> In Fig. 5 the 1-LO-phonon sideband (31.8 meV below the PL peak) for the  $6 \times 90\text{-\AA}^2$  sample is plotted as a function of magnetic field. A clear enhancement of the intensity  $I_{\text{LO}}$  is observed as a function of magnetic field. This behavior can be understood in terms of a semiclassical model<sup>22</sup> where the localized exciton induces polarization of the lattice, giving rise to 1-LO-phonon satellites. The intensity of the 1-LO-plasmon satellite can be written as

$$I_{\text{LO}} \propto \int d^3r |\mathbf{D}(\mathbf{r})|^2, \quad (10)$$

where  $\mathbf{D}(\mathbf{r})$  is the electric displacement due to the exciton charge  $e[n_h(\mathbf{r})-n_e(\mathbf{r})]$ . To describe the physical picture of a correlated electron-hole pair in a QW, whose center

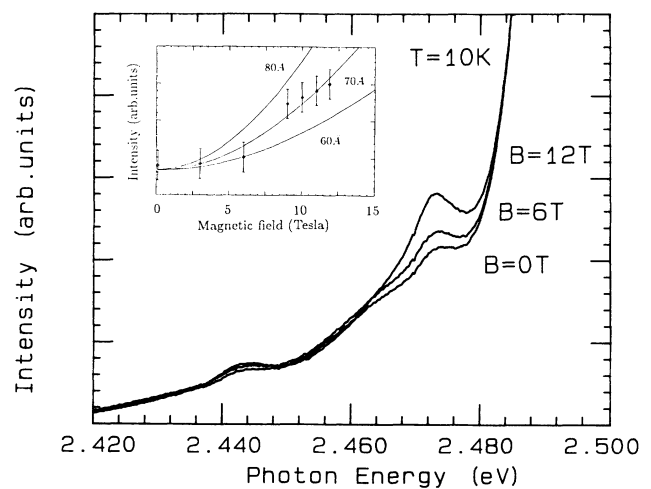


FIG. 5. 1-LO-phonon sideband photoluminescence spectra as a function of magnetic field, for a MQW sample with  $L_w=90\text{ \AA}$ . In the inset the intensity of the 1-LO-phonon sideband vs magnetic field is plotted. The solid lines are theoretical curves for different values of a length parameter expressing the localization radius of the QW exciton as defined in the text.

of mass motion is restricted in a region of the QW plane, it is meaningful to take the electron and hole densities  $n_e$  and  $n_h$  (as in Ref. 22) to be of the form  $n_{1a}(x,y)n_{0a}(z)$ , where  $a=e,h$ ,  $n_{0a}(z)$  are calculated in the envelope-function approximation and  $n_{1a}(x,y)$  are taken as normalized Gaussians with variances  $\langle x_a^2 \rangle = \langle y_a^2 \rangle = \sigma_a^2$ . The quantities  $\sigma_e$  and  $\sigma_h$  represent the radii of localization about the exciton binding center of the electron and hole charges, respectively, and for the purposes of this analysis are taken to be equal to  $\sigma$ . Considering that the  $(\text{Zn,Cd})\text{Se}$  system exhibits one mode behavior and that the  $\hbar\omega_{\text{LO}}(\mathbf{k} \simeq \mathbf{0})$  of the QW material due to the strain effect almost coincides with the  $\hbar\omega_{\text{LO}}$  of the ZnSe barrier layer we take the integration limits to extend over all space. The magnetic-field dependence of the  $I_{\text{LO}}$  comes through the diamagnetic shrinkage of the localized exciton which can be expressed<sup>24</sup> as

$$\sigma^{-4}(B) = \sigma^{-4}(B=0) + l_B^{-4}, \quad (11)$$

where  $l_B = (\hbar/eB)^{1/2}$  is the magnetic length (74 Å at 12T). In the inset of Fig. 5 we plot the calculated 1-LO-phonon satellite intensity as a function of magnetic field for different values of  $\sigma$ . We find that the best match to the data points is obtained for an exciton localization radius of 70 Å. Therefore we conclude that the length-scale over which the exciton in our QW system is localized along the QW plane is of the order of a few exciton-radius lengths. This is also consistent with the fact that the diamagnetic energy shift of the PL peak is identical to that of the exciton absorption peak which probes delocal-

ized excitons. In the case that the exciton localization length were smaller than the Bohr radius of the exciton, the diamagnetic shift would be significantly reduced.<sup>24</sup>

In summary, we have studied the optical properties of quasi-2D excitons in moderately strained  $(\text{Zn,Cd})\text{Se}/\text{ZnSe}$  MQW's, a system which is proving to be quite useful in optoelectronic applications. For samples with small total QW thickness, the strain is accommodated pseudomorphically in the QW layers and provides for additional confinement of the HH excitons. Distinct excitonic absorption features are well preserved at room temperature and beyond, demonstrated here in a ZnSe-based system. The exciton-LO-phonon coupling, the main cause of temperature-dependent broadening, is reduced in samples with narrow QW widths. This is explained in terms of a model where quasi-2D confinement effects increase the exciton binding energy to a value greater than the LO-phonon energy and hence reduces the available phase space for the exciton-LO-phonon scattering process. Magnetotransmission experiments offer direct evidence that  $R_y^* > \hbar\omega_{\text{LO}}$ . Finally, magnetoluminescence experiments indicate that excitons become localized in areas of QW imperfections that span a few exciton diameters.

This work was carried out in part at Francis Bitter National Magnet Laboratory at MIT which is supported by the National Science Foundation. The work at Brown University and University of Notre Dame was supported by the NSF and the Defense Advanced Research Projects Agency.

- 
- <sup>1</sup>M. A. Haase, J. Qiu, J. M. Depuydt, and H. Cheng, *Appl. Phys. Lett.* **59**, 1272 (1991); H. Jeon, J. Ding, W. Xie, M. Kobayashi, R. L. Gunshor, and A. V. Nurmikko, *Appl. Phys. Lett.* **59**, 3619 (1991).
- <sup>2</sup>J. Ding, N. Pelekanos, A. V. Nurmikko, H. Luo, N. Samarth, and J. K. Furdyna, *Appl. Phys. Lett.* **57**, 2885 (1990).
- <sup>3</sup>See, D. Chemla, S. Schmitt-Rink, and D. A. B. Miller, in *Optical Nonlinearities and Instabilities in Semiconductors*, edited by H. Haug (Academic, New York, 1988), p. 83.
- <sup>4</sup>S. Rudin, T. L. Reinecke, and B. Segall, *Phys. Rev. B* **42**, 11 218 (1990).
- <sup>5</sup>N. Pelekanos, J. Ding, and A. V. Nurmikko (unpublished).
- <sup>6</sup>N. Samarth, H. Luo, J. K. Furdyna, R. G. Alonso, Y. R. Lee, A. K. Ramdas, S. B. Qadri, and N. Otsuka, *Appl. Phys. Lett.* **56**, 1163 (1990).
- <sup>7</sup>M. Ya. Valakh, M. P. Lisitsa, G. S. Pekar, G. N. Polysskii, V. I. Sidorenko, and A. M. Yaremko, *Phys. Status Solidi B* **113**, 635 (1982).
- <sup>8</sup>F. Cerdeira, C. J. Buchenauer, F. H. Pollack, and M. Cardona, *Phys. Rev. B* **5**, 580 (1972).
- <sup>9</sup>W. Walecki, A. V. Nurmikko, N. Samarth, H. Luo, J. K. Furdyna, and N. Otsuka, *Appl. Phys. Lett.* **57**, 446 (1990).
- <sup>10</sup>C. G. Van de Walle, *Phys. Rev. B* **39**, 1871 (1989).
- <sup>11</sup>C. Weisbuch, R. Dingle, A. C. Gossard, and W. Wiegmann, *Solid State Commun.* **38**, 709 (1981).
- <sup>12</sup>R. Zimmermann, *J. Cryst. Growth* **101**, 346 (1990).
- <sup>13</sup>J. Lee, E. Koteles, and M. O. Vassell, *Phys. Rev. B* **33**, 5512 (1986).
- <sup>14</sup>J. S. Wiener, D. S. Chemla, D. A. B. Miller, T. H. Wood, D. Sivco, and A. Y. Cho, *Appl. Phys. Lett.* **46**, 619 (1985).
- <sup>15</sup>D. S. Chemla, D. A. B. Miller, P. W. Smith, A. C. Gossard, and W. Wiegmann, *IEEE J. Quantum Electron.* **QE-20**, 265 (1984).
- <sup>16</sup>O. Akimoto and H. Hasegawa, *J. Phys. Soc. Jpn.* **22**, 181 (1966).
- <sup>17</sup>H. W. Hölscher, A. Nöthe, and C. Uihlein, *Phys. Rev. B* **31**, 2379 (1985).
- <sup>18</sup>A. Fasolino and M. Altarelli, *Two Dimensional Systems, Heterostructures, and Superlattices*, edited by G. Bauer, F. Kuchar, and H. Heinrich, Springer Series in Solid State Sciences Vol. 53 (Springer, New York, 1984), p. 176.
- <sup>19</sup>R. L. Greene and K. K. Bajaj, *Phys. Rev. B* **31**, 6498 (1985).
- <sup>20</sup>M. Kumagai and T. Takagahara, *Phys. Rev. B* **40**, 12 359 (1989); T. Thoai, R. Zimmermann, M. Grundmann, and D. Bimberg, *ibid.* **42**, 5906 (1990).
- <sup>21</sup>J. Ding, H. Jeon, T. Ishihara, A. V. Nurmikko, H. Luo, N. Samarth, and J. K. Furdyna, in *Proceedings of the Conference on Modulated Semiconductor Structure V*, Nara, Japan, 1991, [Surf. Sci. (to be published)]; J. Ding, H. Jeon, T. Ishihara, A. V. Nurmikko, H. Luo, N. Samarth, and J. K. Furdyna (unpublished).
- <sup>22</sup>K. J. Nash, M. S. Skolnick, P. A. Claxton, and J. S. Roberts, *Phys. Rev. B* **39**, 5558 (1989).
- <sup>23</sup>J. J. Hopfield, *J. Phys. Chem. Solids* **10**, 110 (1959).
- <sup>24</sup>K. J. Nash, M. S. Skolnick, P. A. Claxton, and J. S. Roberts, *Phys. Rev. B* **39**, 10 943 (1989).

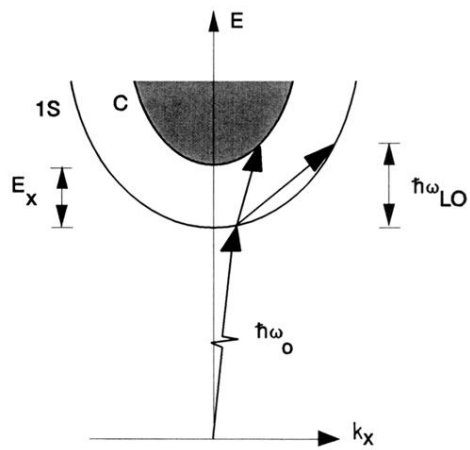


FIG. 1. Schematic illustration of the major processes (arrows) contributing to the phonon induced lifetime of the lowest-lying exciton. The shaded area represents continuum states.